crystals

MDPI

Article

A Fast-Response and Helicity-Dependent Lens Enabled by Micro-Patterned Dual-Frequency Liquid Crystals

Wei Duan [1], Peng Chen [1,3], Shi-Jun Ge [1,3], Xiao Liang [2,*] and Wei Hu [1,3,*]

[1] Key Laboratory of Intelligent Optical Sensing and Manipulation, College of Engineering and Applied Sciences, Nanjing University, Nanjing 210093, China; dwlightnju@126.com (W.D.); ndclchuangxinjihua@163.com (P.C.); geshijun@nju.edu.cn (S.-J.G.)
[2] Department of Chemistry, Tsinghua University, Beijing 100084, China
[3] Institute for Smart Liquid Crystals, JITRI, Changshu 215500, China
[*] Correspondence: liangxiao@tsinghua.edu.cn (X.L.); huwei@nju.edu.cn (W.H.); Tel.: +86-25-83597400 (X.L. & W.H.)

Received: 7 January 2019; Accepted: 16 February 2019; Published: 20 February 2019

Abstract: Liquid crystals are excellent candidates for tunable optical elements due to their large birefringence and continuous tunability by external fields. A dual-frequency liquid crystal lens integrated with Pancharatnam–Berry phase was fabricated via a dynamic photo-patterning technique. The proposed lens exhibited distinctive polarization-dependent characteristics and ultra-high efficiency rates of up to 95%. Via merely alternating the frequency of the applied electric field, the switching time between unfocused and focused states was measured in submilliseconds. This work supplies a new strategy for fast-response, high-efficiency and helicity-dependent lens with merits of easy fabrication and low power consumption.

Keywords: diffractive lens; Pancharatnam–Berry phase; dual-frequency liquid crystals; patterned photoalignment

1. Introduction

Nowadays, liquid crystals (LCs) have experienced rapid development due to their pronounced optical anisotropy and continuous external field tunability and have become prospective candidates for tunable diffractive optical elements. Adaptive LC lenses have been developed to be a useful type of diffractive element, and play vitally important roles in the development of machine vision, ophthalmic apparatuses, augmented reality display fields, etc. [1–3]. Several practical LC techniques, such as zone-patterned structures [4], hole or hybrid-patterned electrodes [5–9], and inhomogeneous polymer networks [10], have been proposed for lens fabrication.

The applications of these electrically-tunable LC lenses are determined by two key parameters, switching time and optical efficiency. To improve the switching responsiveness, several kinds of LCs with fast-responsive characteristics, such as ferroelectric LCs, blue-phase LCs, dual-frequency LCs (DFLCs) and polymer-dispersed LCs [11–13] have been employed. However, the delicate electrodes and inhomogeneous materials are only suitable for the generation of binary phase profiles [2], and the diffraction efficiency of a LC lens is severely restricted. Moreover, the complex fabrication makes these strategies costly and inefficient. By introducing orthogonal azimuthal angle control of LCs, realized by a photoalignment technique, Fresnel lenses, with their diffraction efficiencies improved to 40.5%, are presented [14]. More recently, the Pancharatnam–Berry (PB) phase has been integrated to realize a continuous lens phase profile, thus pushing the theoretical limit to 100% [15]. If one can supply a simple and efficient way for fabricating PB lenses with fast response LCs, the two key requirements could be satisfied simultaneously.

Here, a polarization lens based on DFLC is demonstrated by introducing a PB phase [16], which can greatly improve the experimental diffractive efficiency up to 95%. The designed PB lens is an inhomogeneous LC wave plate, in which optical axis distribution is dependent on the designed focal length (F) and the free space wavelength (λ). A dynamic microlithography system with a LC photo-patterning technique is utilized for the PB lens preparation to realize continuously variant director distributions. By merely alternating the frequency of the applied external electric field, the switching time between transformed-focused state and remained-unfocused state reaches the submillisecond scale. In addition, the focusing/defocusing characteristics are determined by the helicity of the incident light. This work provides a practical strategy for high-efficiency and fast-responsive optical diffractive elements.

2. Principles and Experiments

2.1. Principles

A PB lens can locally modulate the incident polarization states and results in a space-variant output phase, namely the PB phase [17]. The PB phase results from the space-variant manipulation of polarization states. A typical design using the PB phase concept relies on laterally inducing different polarization variations of a propagating beam, which can be realized by inhomogeneous anisotropic media, such as LCs. The designed optical axes of a DFLC PB lens are homogeneous along the z axis in the LC cell and obey the equation on both substrates (defined as the x-y-coordinate axis):

$$\alpha = \frac{\pi}{\lambda}\left(\sqrt{r^2 + F^2} - F\right) \tag{1}$$

where α is the LC azimuthal angle, r is the radius corresponding to the x-y coordinates, $r^2 = x^2 + y^2$, F stands for the designed focal length and λ indicates the free-space wavelength. Figure 1 shows the simulated director distribution of the PB lens structure with the theoretically designed focal length being F = 10 cm (for λ = 671 nm). The continuous color changes from blue to red indicate that the optical axis orientation of the desired PB lens continuously changes from 0 to π.

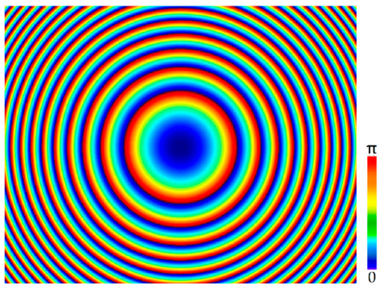

Figure 1. The simulated director distribution of the Pancharatnam–Berry phase lens.

The property of the helicity-dependent diffraction can be theoretically derived by the Jones matrix calculation. The transformation in a PB lens can be analyzed as follows:

$$\begin{aligned}\mathbf{T} &= \mathbf{R}(-\alpha)\cdot\begin{bmatrix}\exp(-i\Gamma/2) & 0\\ 0 & \exp(i\Gamma/2)\end{bmatrix}\cdot\mathbf{R}(\alpha)\\ &= \cos\tfrac{\Gamma}{2}\mathbf{I} - i\sin\tfrac{\Gamma}{2}\begin{bmatrix}\cos 2\alpha & \sin 2\alpha\\ \sin 2\alpha & -\cos 2\alpha\end{bmatrix}\end{aligned} \tag{2}$$

where $\Gamma = 2\pi\Delta n d/\lambda$ is the phase retardation, Δn is the LC birefringence, and d indicates the LC cell gap. Considering a right/left circular polarized input light, which can be described as

$\mathbf{E}_{\text{in}} = \chi^{(\pm)} = 1/\sqrt{2}\begin{pmatrix} 1 & \pm i \end{pmatrix}^{\mathrm{T}}$, the two spin eigenstates denote the left (+) and right (−) circular polarization states. After passing through the LC PB lens, the output can be expressed after applying the transformed matrix:

$$\mathbf{E}_{out} = \mathbf{T} \cdot \mathbf{E}_{\text{in}} = \cos\frac{\Gamma}{2} \cdot \chi^{(\pm)} - i\sin\frac{\Gamma}{2} \cdot \exp\left[\pm i\frac{2\pi}{\lambda}\left(\sqrt{r^2 + F^2} - F\right)\right] \cdot \chi^{(\mp)} \quad (3)$$

When the incident is a right circular polarized (RCP) beam, the output can be taken as two parts: The residual RCP component, and the transformed left circular polarized (LCP) part, added to a spherical phase factor $\exp\{-i2\pi[(r^2 + F^2)^{1/2} - F]/\lambda\}$ resulting in a concave spherical wavefront. As a consequence, the input RCP can be transformed into a focused LCP. On the contrary, for an LCP incident beam, the defocused transformed RCP can be obtained. Only when the phase retardation satisfies the half-wave condition, i.e., $\Gamma = (2n + 1)\pi$ (n is an integer), can the residual part be totally suppressed and the obtained output is a pure focused/defocused beam. In this case, for a circular polarization incident, it will theoretically be 100% transformed into a focused/defocused state.

For common nematic LCs, when the electric field is switched off, the relaxing time of LCs return to the original state is determined by the alignment conditions, as well as the LCs intrinsic elastic and viscosity properties, which can reach the tens of milliseconds scale. DFLC is a kind of LC mixture with opposite dielectric anisotropy [18,19]. It exhibits a positive dielectric anisotropy ($\Delta\varepsilon > 0$) when the applied electric field frequency is below f_c (defined as crossover frequency). It becomes negative ($\Delta\varepsilon < 0$) at the frequency $f > f_c$. When an appropriate external electric field with $f > f_c$ is applied, the LC directors orient perpendicularly to the electric field direction. While $f < f_c$, the LC director orientation tends to be parallel to the electric field. This phenomenon enhances the LC's responsive ability by merely alternating the applied frequency at a relatively low voltage, enabling the possibility of a submillisecond scale response.

2.2. Setup and Experiments

The orange lines in Figure 2a schematically show the director distribution of a PB lens. The dark domains under the crossed polarizers correspond to regions with LC directors approximately parallel or perpendicular to the polarizer, whereas the bright domains correspond to regions with LC directors around ±45° with respect to the polarizer. Figure 2b presents a micrograph image of a DFLC PB lens sample with designed F = 10 cm (for λ = 671 nm) observed under a cross-polarized optical microscope. The continuous variation of the brightness and darkness gives a vivid exhibition of the space-variant directors. When rotating the sample, the bright and dark domains interconvert gradually, further manifesting the continuous space variant of the directors. As the cell gap d is experimentally optimized to make the phase retardation satisfy the half-wave condition, the light is totally focused (i.e., On state). When the phase retardation approximates zero because the DFLC is driven by a low frequency signal, the unfocused state (i.e., Off state) is obtained. It can be turned to the On state rapidly with a high frequency signal.

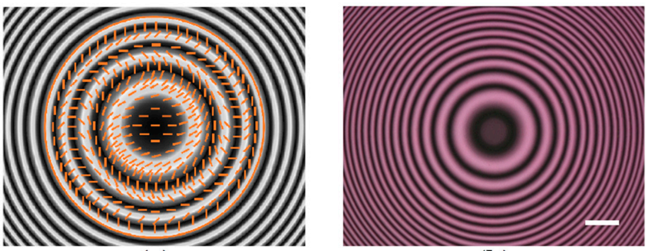

(**a**) (**b**)

Figure 2. (**a**) Schematic director distributions and (**b**) the corresponding micrograph of the DFLC PB lens with F = 10 cm. The scale bar is 200 μm.

To characterize the diffractive performance of the PB lens, an experimental optical setup for generating and analyzing focused/defocused beams was built, as illustrated in Figure 3. As shown in Figure 3, a 671 nm laser beam passes through a polarizer and then a quarter wave-plate (QWP), and then illuminates on the sample and finally is captured by a Charge Coupled Device (CCD). The angle between the polarization direction and the *c*-axis of the QWP was set to be +45°/−45° to control the incident RCP/LCP polarization, respectively. The transformed output focused/defocused beams are thus generated.

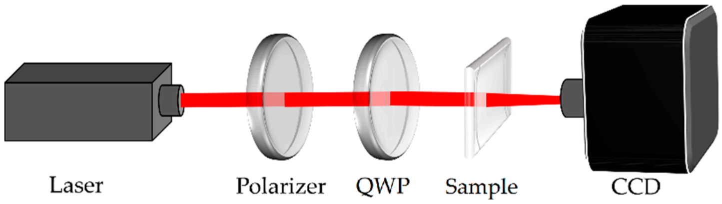

Figure 3. The optical setup for characterizing the performance of the PB lens.

3. Results and Discussion

The microscope images of the PB lens under crossed polarizers at an applied voltage 25 V with frequencies of 1 kHz and 65 kHz are shown in Figure 4a,b. When a 671-nm incident RCP passes through the sample, the transmitted pattern is shown in Figure 4c. A Gaussian-like beam is observed in the center, and the variant colors indicate the intensity. In this situation, the applied voltage was 25 V with a frequency of 1 kHz below f_c (the f_c was measured as 40 kHz at this voltage). Thus, the LCs tend to orient parallel to the external field and have an isotropic effect on the incident light. This can also be observed for the LCP condition. The obtained output light stays the same as the incident state (unfocused state), which can be defined as the Off state. When applying a high-frequency electric field (25 V, 65 kHz), the LCs tend to reorient perpendicularly to the electric field (i.e., parallel to the substrates) and hold gradiently variant orientations, forming the focused state (i.e., On state) as shown in Figure 4d. Figure 4e reveals that a defocused diffracted beam has been generated on the concentric position for an LCP incident beam when merely alternating the *c*-axis orientation of the QWP and keeping the external field unchanged. Figure 4d,e indicate that the PB lens is helicity-dependent, inducing a concave/convex spherical wavefront to the RCP/LCP, respectively. Thus, a focused/defocused beam is obtained. As expected, for a linear-incident polarization, the two circularly polarized beam components are equally diffracted to both focused and defocused states, as shown in Figure 4f. Thus, switching between two focused/defocused states could be realized by merely adjusting the incident polarization. In addition, the measured focal length is F = 10.11 cm, which approximates the designed value.

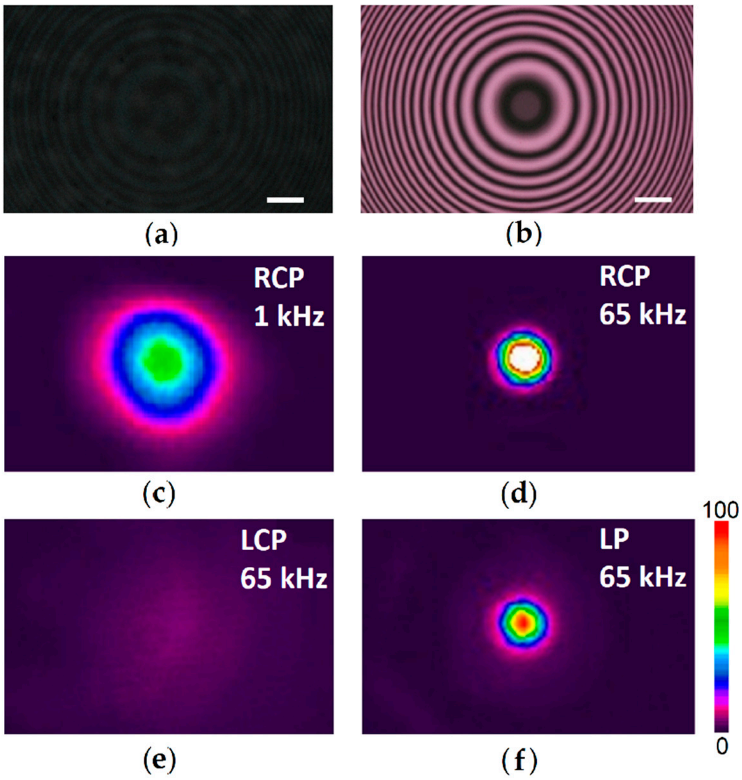

Figure 4. The microscope images of the PB lens under crossed polarizers in the applied voltage 25 V with the frequency of (**a**) 1 kHz and (**b**) 65 kHz, and the images of diffraction patterns at 25 V, 1 kHz of (**c**) right circular polarization (RCP), and at 25 V, 65 kHz of (**d**) RCP, (**e**) left circular polarization (LCP) and (**f**) linearly polarized incident beams. The scale bar is 200 μm. The colored scale bar shows the normalized intensity gradient.

Therefore, while keeping these voltages, the switching between On/Off states could be realized by merely alternating the frequency. As a key parameter of a diffractive element, the switching time is measured. Since a larger voltage quickens the response [20], the switching performance of the PB lens sample is measured by applying an external electric field of 25 V. Furthermore, the major challenge of DFLC devices is the noticeable dielectric-heating effect originating from the applied high frequency, which in turn causes the f_c to drift [21,22]. The f_c satisfies the Arrhenius equation, and is proportional to $\exp(-E/k_B T)$, where k_B is the Boltzmann's constant, and T is the absolute temperature. The f_c increases with the increasing of T [23]. In our experiments, the measured f_c was 40 kHz. DFLC dielectric constant $\Delta\varepsilon$ was 4.2 at 1 kHz, while it shifted to -3.1 at 65 kHz. When the frequency was over 100 kHz, $\Delta\varepsilon$ maintained a constant value of -3.5. A higher frequency will induce a more serious thermodielectric effect, which leads to an instability of crossover frequency. To minimize the thermodielctric effect, the frequency was set at 65 kHz. In order to get a precise measurement, we added a tunable aperture (the diameter set at 0.40 millimeters) before the optical power detector, and adjusted it to an appropriate position to ensure that the focused beam could completely pass through it, while only a very small amount of the unfocused beam passes. As illustrated in Figure 5, a 25 V alternating voltage was applied with frequency interconverting of 1 kHz and 65 kHz, and lasting for 5 ms each signal cycle. The switching times between focused/unfocused states (defined as the duration time that intensity changes from 10% maximum to 90% maximum and reverse) were measured as 680 μs and 550 μs, respectively. Thus, submillisecond switching processes were achieved.

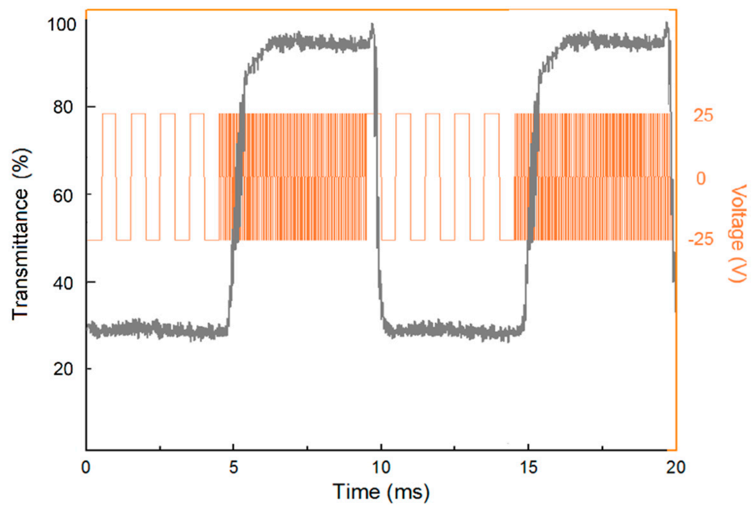

Figure 5. The switching response of the sample (gray line) to the applied signals (orange line).

Response performance could be further improved by increasing voltages or reducing the cell gap. By introducing a linearly gradient phase, the focused and defocused states can be spatially separated to two focal points with one beam focused and the other diverged. Moreover, the transformed focused/defocused states can be distinguished with the unfocused state [24]. Though a simple PB lens is demonstrated in this work, it provides a strategy for realizing optical elements with more complicated and fantastic structures.

4. Materials and Methods

Photoalignment is suitable for high-quality LC alignment. Here, a polarization-sensitive medium, sulfonic azo dye SD1 (Dai-Nippon Ink and Chemicals, Japan), was utilized as the photoalignment agent. When a linearly polarized UV is incident onto the alignment layer, SD1 molecules tend to reorient their absorption oscillators perpendicular to the polarization direction in order to minimize photon absorption [25], consequently guiding the LC orientations owing to the excellent fluidity and continuity of LC.

A digital micro-mirror device-based dynamic microlithography system [26] was utilized to perform the photo-patterning on SD1 (0.3% solution in dimethylformamide) spin-coated indium-tin-oxide glass substrates (1.5 × 2 cm^2, 1.1 mm thickness). The substrates were ultrasonically bathed, UV-ozone cleaned and cured at 100 °C for 10 minutes in advance. To satisfy the half-wave condition for λ = 671 nm, spacers 5 μm in diameter were selected to keep the cell gap. One substrate covered with spurted spacers and a counter one were put together and sealed by epoxy glue to form the cell. Then, the cell was placed at the image plane of the microlithography system to record the designed PB lens pattern. After an eighteen-step five-time-partly-overlapping UV exposure [27], a quasi-continuous space-variant orientation of SD1 was carried out. When the DFLC (HEF951800100, HCCH, China. Δn = 0.206 at λ = 671 nm) is capillarily filled, a polarization lens was accomplished.

5. Conclusions

In this work, we proposed and demonstrated a high-efficiency and fast-response DFLC polarization lens via a dynamic photo-patterning technique. The switching between focused/defocused states and focused/unfocused states can be realized by alternating the incident polarization and the frequency of certain applied electric field, respectively. A high diffraction efficiency of up to 95% is obtained for a focused state with a circular polarization incident. Via merely alternating the frequency of applied electric field, the response time between focused and unfocused states reach 680 μs and 550 μs, respectively, both of which are in the submillisecond scale. It supplies a new design for high-efficiency and fast-response optical diffractive lens with the merits of easy fabrication and low power consumption. It may also broaden LC lens applications in integrated optics, information processing, optical communications, and other fields.

Author Contributions: W.H. conceived the original idea; W.D., P.C., and S.-J.G. performed the experiments, analyzed the data and wrote the manuscript; X.L. performed a constructive analysis of the DFLC material; W.H. supervised and directed the research.

Funding: This work was sponsored by the Distinguished Young Scholars Fund of Jiangsu Province (BK20180004), the National Natural Science Foundation of China (Nos. 61575093, 61535007 and 61435008) and Jiangsu Donghai Silicon Industry Science and Technology Innovation Center.

Acknowledgments: The authors are indebted to V. Chigrinov for his kind support with the photoalignment technique. W.H. gratefully acknowledges the support of the Tang Scholar program.

Conflicts of Interest: The authors declare no conflict of interest.

References

1. Sato, S. Liquid-crystal lens-cells with variable focal length. *Jpn. J. Appl. Phys.* **1979**, *18*, 1679–1684. [CrossRef]
2. Ren, H.; Wu, S.T. *Introduction to Adaptive Lenses*; John Wiley & Sons: Hoboken, NJ, USA, 2012; Volume 75.
3. Lin, Y.H.; Chen, H.S. Electrically tunable-focusing and polarizer-free liquid crystal lenses for ophthalmic applications. *Opt. Express* **2013**, *21*, 9428–9436. [CrossRef] [PubMed]
4. Patel, J.S.; Rastani, K. Electrically controlled polarization-independent liquid-crystal Fresnel lens arrays. *Opt. Lett.* **1991**, *16*, 532–534. [CrossRef] [PubMed]
5. Nose, T.; Masuda, S.; Sato, S. A liquid crystal microlens with hole-patterned electrodes on both substrates. *Jpn. J. Appl. Phys.* **1992**, *31*, 1643–1646. [CrossRef]
6. Nose, T.; Masuda, S.; Sato, S.; Li, J.; Chien, L.C.; Bos, P.J. Effects of low polymer content in a liquid-crystal microlens. *Opt. Lett.* **1997**, *22*, 351–353. [CrossRef]
7. Klaus, W.; Ide, M.; Hayano, Y.; Morokawa, S.; Arimoto, Y. Adaptive LC lens array and its application. *Proc. SPIE* **1999**, *3635*, 66–73. [CrossRef]
8. Kao, Y.Y.; Chao, P.P. A new dual-frequency liquid crystal lens with ring-and-pie electrodes and a driving scheme to prevent disclination lines and improve recovery time. *Sensors* **2011**, *11*, 5402–5415. [CrossRef]
9. Choi, Y.; Choi, T.H.; Woo, J.-H.; Jeon, B.G.; Yoon, T.H. Fast turn-off switching of vertically-aligned negative liquid crystals by fine patterning of pixel electrodes. *Crystals* **2017**, *7*, 201. [CrossRef]
10. Ren, H.; Fan, H.Y.; Gauza, S.; Wu, S.T. Tunable microlens arrays using polymer network liquid crystal. *Opt. Commun.* **2004**, *230*, 267–271. [CrossRef]
11. Li, Y.; Wu, S.T. Polarization independent adaptive microlens with a blue-phase liquid crystal. *Opt. Express* **2011**, *19*, 8045–8050. [CrossRef]
12. Pishnyak, O.; Sato, S.; Lavrentovich, O.D. Electrically tunable lens based on a dual-frequency nematic liquid crystal. *Appl. Opt.* **2006**, *45*, 4576–4582. [CrossRef]
13. Ren, H.; Fan, Y.H.; Wu, S.T. Liquid-crystal microlens arrays using patterned polymer networks. *Opt. Lett.* **2004**, *29*, 1608–1610. [CrossRef] [PubMed]
14. Wang, X.; Fan, F.; Du, T.; Tam, A.M.W.; Ma, Y.; Srivastava, A.K.; Chigrinov, V.; Kwok, H. Liquid crystal Fresnel zone lens based on single-side-patterned photoalignment layer. *Appl. Opt.* **2014**, *53*, 2026–2029. [CrossRef] [PubMed]
15. Tabiryan, N.V.; Serak, S.V.; Nersisyan, S.R.; Roberts, D.E.; Zeldovich, B.Y.; Steeves, D.M.; Kimball, B.R. Broadband waveplate lenses. *Opt. Express* **2016**, *24*, 7091–7102. [CrossRef]
16. Duan, W.; Chen, P.; Wei, B.Y.; Ge, S.J.; Liang, X.; Hu, W.; Lu, Y.Q. Fast-response and high-efficiency optical switch based on dual-frequency liquid crystal polarization grating. *Opt. Mater. Express* **2016**, *6*, 597–602. [CrossRef]
17. Berry, M.V. The adiabatic phase and Pancharatnam's phase for polarized light. *J. Mod. Opt.* **1987**, *34*, 1401–1407. [CrossRef]
18. Schadt, M. Low-frequency dielectric relaxations in nematics and dual-frequency addressing of field effects. *Mol. Cryst. Liq. Cryst.* **1982**, *89*, 77–92. [CrossRef]
19. Xianyu, H.; Wu, S.T.; Lin, C.L. Dual frequency liquid crystals: A review. *Liq. Cryst.* **2009**, *36*, 717–726. [CrossRef]
20. Khoo, C.; Wu, S.T. *Optics and Nonlinear Optics of Liquid Crystals*; World Scientific: Singapore, 1993.

21. Wen, C.H.; Wu, S.T. Dielectric heating effects of dual-frequency liquid crystals. *Appl. Phys. Lett.* **2005**, *86*, 231104. [CrossRef]
22. Hsiao, Y.C.; Lee, W. Lower operation voltage in dual-frequency cholesteric liquid crystals based on the thermodielectric effect. *Opt. Express* **2013**, *21*, 23927–23933. [CrossRef]
23. Hsiao, Y.C.; Tang, C.Y.; Lee, W. Fast-switching bistable cholesteric intensity modulator. *Opt. Express* **2011**, *19*, 9744–9749. [CrossRef] [PubMed]
24. Duan, W.; Chen, P.; Ge, S.J.; Wei, B.Y.; Hu, W.; Lu, Y.Q. Helicity-dependent forked vortex lens based on photo-patterned liquid crystals. *Opt. Express* **2017**, *25*, 14059–14064. [CrossRef] [PubMed]
25. Chigrinov, V.; Pikin, S.; Verevochnikov, A.; Kozenkov, V.; Khazimullin, M.; Ho, J.; Huang, D.D.; Kwok, H.S. Diffusion model of photoaligning in azo-dye layers. *Phys. Rev. E* **2004**, *69*, 061713. [CrossRef] [PubMed]
26. Wu, H.; Hu, W.; Hu, H.C.; Lin, X.W.; Zhu, G.; Choi, J.W.; Chigrinov, V.; Lu, Q.Y. Arbitrary photo-patterning in liquid crystal alignments using DMD based lithography system. *Opt. Express* **2012**, *20*, 16684–16689. [CrossRef]
27. Chen, P.; Wei, B.Y.; Ji, W.; Ge, S.J.; Hu, W.; Xu, F.; Chigrinov, V.; Lu, Y.Q. Arbitrary and reconfigurable optical vortex generation: A high-efficiency technique using director-varying liquid crystal fork gratings. *Photonics Res.* **2015**, *3*, 133–139. [CrossRef]